PROCEEDINGS OF SCIENCE

The LHC Radiation Monitoring System - RadMon

Giovanni Spiezia
CERN
CERN CH-1211, Genève 23, Switzerland
E-mail: Giovanni.Spiezia@cern.ch

Julien Mekki[1], Sergio Batuca, Markus Brugger, Marco Calviani, Alfredo Ferrari, Daniel Kramer, Roberto Losito, Alessandro Masi, Anna Nyul, Paul Peronnard, Christian Pignard, Ketil Roeed, Thijs Wijnands
CERN
CERN CH-1211, Genève 23, Switzerland
E-mail: ; Julien.Mekki@cern.ch; Sergio.batuca@cern.ch; Markus.Brugger@cern.ch; Marco.Calviani@cern.ch, Alfredo.Ferrari@cern.ch; Daniel.kramer@cern.ch; Roberto.Losito@cern.ch; Alessandro.Masi@cern.ch; Ana.Nyul@cern.ch; Paul.Peronnard@cern.ch; Christian.Pignard@cern.ch; Ketil.Roeed@cern.ch; Thijs.Wijnands@cern.ch

The Large Hadron Collider (LHC) is a complex radiation environment consisting of several particle types at different energies that affects the electronic equipments. The Radiation Monitoring System, hereafter RadMon, is designed to measure the radiation effects on the electronics in the LHC tunnel and its adjacent shielded areas in order to monitor the radiation levels, anticipate possible device degradation and identify instantaneous failures of the electronic equipments, correlated to their typical Mean Time Between Failure (MTBF) as caused by radiation. The RadMon monitoring aims also to validate the FLUKA Monte-Carlo calculations of the radiation environment as used to predict present and future radiation levels expected for the LHC. For these purposes, the RadMon provides the measurement of the Total Ionizing Dose (TID) in Silicon dioxide by means of Radiation-sensing Field-Effect Transistors (RadFETs), of the Displacement Damage (DD) in Silicon by means of p-i-n diodes, and of the High Energy Hadrons (HEH) and thermal neutrons fluence by counting Single Events Upsets (SEU) in SRAM memory.

10th International Conference on Large Scale Applications and Radiation Hardness of Semiconductor Detectors
Firenze, Italy
July 6-8, 2011
[1] Speaker

1. Introduction

A reliable monitoring system is required for the precise operation of accelerators, and a detailed knowledge of the radiation field in the accelerator tunnel and adjacent areas is important in order to design installation, relocation or shielding requirements of electronics sensitive to radiation. Monitoring system for accelerators is optimized to allow for proper beam steering and the detection of beam losses, with limited performance for the measurement of the radiation fields and respective quantities important for radiation damage issues. For this reason the RadMon system has been developed by the CERN ENgineering (EN) department [1]. The RadMon system includes RadFETs for Total Ionising Dose (TID) measurements, silicon p-i-n diodes for the 1-MeV equivalent neutron fluence, and SRAM memories for the high energy hadron and thermal neutron fluence. Given the nature of high-energy accelerators and their operation principles, radiation sources can be grouped into three main categories: (a) direct losses in collimator and absorber like objects, (b) particle debris from beam collisions in the four main experiments, and (c) interaction of the beam with the residual gas inside the beam pipe. The variety of source terms results in a unique radiation field of mixed particle types and energies, as shown in Fig. 1, for a typical LHC tunnel area. Inside the accelerator tunnel protons and pions contribute to the largest fraction of the high-energy hadron fluence which is source term for Single Event Effects (SEEs), which can be non-destructive events, such as for instance Single Event Upsets (SEUs) in SRAM memories, or destructive events, such as Single Event Latchup (SEL) in mixed signal devices, or Single Event Burnout (SEB) in power switches. Conversely, neutrons are the main source term in the adjacent and partly shielded areas. In the following section, the measurement methodologies of the different sensors used on the RadMon are described. In addition, the software architecture to retrieve and store the data is detailed. In section 4, applications of the RadMon system in CERN experimental test areas, used for radiation tests (CNRAD and H4IRRAD) and in the LHC accelerator, are presented.

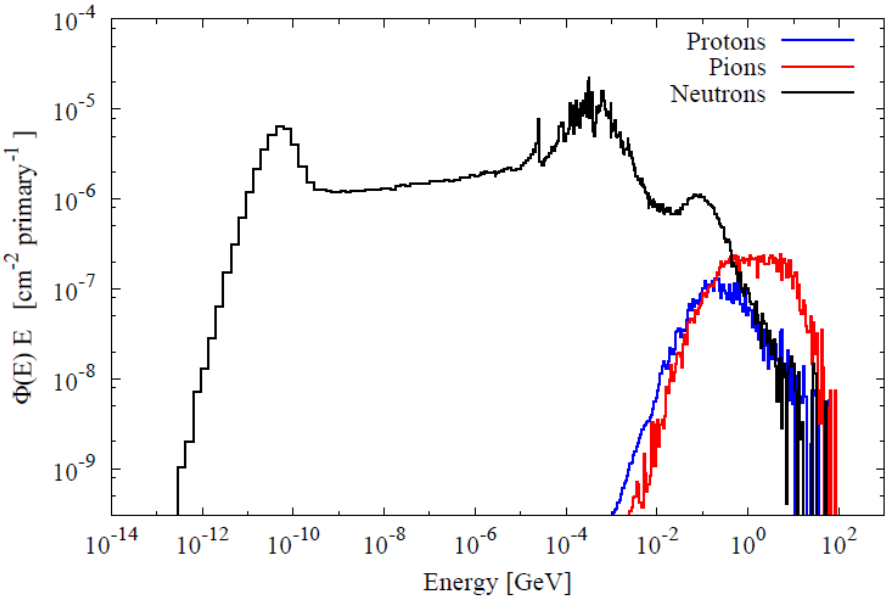

Fig. 1: Particle energy spectra (lethargy) representative for tunnel areas in the LHC.

2.Measurement methodology

A RadMon (20 × 20 × 10 cm^3) measures the radiation levels at its own position. Its sensor window (exposition of RadFETs, p-i-n diodes, and memories) is 5×10 cm^2. Then, the variation of the levels around its location depends on the radiation field itself. For this reason several agents (RadMons) are used in the LHC tunnel zone (27 km) to assure a good coverage of all the areas where sensitive electronics are installed. In the following, the methodology to measure the Total Ionizing Dose, the Displacement Damage, and the Single Event Upsets is described.

2.1Total Ionising Dose - RadFET

RadFETs are p-channel MosFETs which are optimized for monitoring the TID on Electronic Devices [2]. The RadFET dosimeters operate by the build-up of oxide positive trapped charge in the gate silicon oxide layer of the transistor. This positive trapped charged is responsible of the threshold voltage shift (V_{th}) of the transistor, which is measured at a constant drain to source current (I_{ds}). Therefore the growth of the voltage V_{th} is a function of the dose. The variation of the V_{th} at increasing the dose determines the sensitivity of the RadFETs. The sensor reaches the saturation condition when the threshold voltage V_{th} does not vary anymore at increasing the dose. The sensitivity and the saturation conditions depend on the biasing of the gate and on the oxide thickness. As far as the reading circuit is concerned, the RadFETs are used in the LHC accelerator [1] and experiments [3] in "zero bias mode", i.e. the gate is shortcircuited to the ground during irradiation. The reading circuit, described in [1], injects a current pulse I_{ds} of duration of 30 ms, each 1 second, and the tension V_{sg}, representing the V_{th}, is read. The gate and the drain are short-circuited to the ground (V_g= V_d = 0V) during the irradiation and in reading mode. By doing so, as the electric field within the oxide is almost null, the probability for holes to escape recombination effects is small compared to a biased RadFETs ($V_g \neq 0V$). The "zero bias mode" implies that the sensor sensitivity is less than the one which would be obtained by applying a polarization on the gate. Conversely, the measurement range is enlarged since the saturation condition of the RadFET is reached at higher dose. The larger the oxide is, the higher the sensitivity is. The larger the oxide thickness, the lower the measurement range, since the saturation condition is reached at lower dose. The RadMon in the

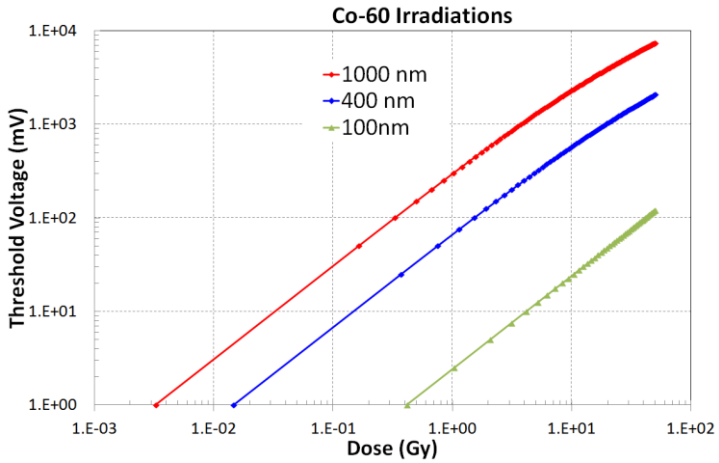

Fig. 2: Radiation responses of the 1000 nm, 400nm and 100 nm (in red, blue and green respectively) during Co-60 gamma irradiations. The RadFET's threshold voltage is plotted versus dose in Gy(Si).

LHC uses three RadFETs with different oxide thickness, 100 nm, 400nm, and 1000nm in order to have three different sensitivities (from about 3 mV/Gy to 240 mV/Gy) and three measurement ranges which allow covering a dose span from 0 Gy to ≈ 5 kGy. Finally, another aspect to consider is the damage annealing effect which is more pronounced on thicker oxides [3]. However, the impact of the annealing effect on the measurement is more evident in the range of higher doses where RadFETs with thinner thickness are used as a countermeasure. The variation of the threshold voltage is depicted as a function of the dose (Gy[Si]) for the 1000 nm, 400nm and 100 nm RadFETs in Fig. 2. The radiation response of the RadFETs is not a linear function of the dose, therefore a quadratic polynom in the form of Eq.1 is used to convert the variation of the threshold voltage with respect to its initial value at 0 Gy, ΔV_{th}, in the dose *D*.

$$D = a \times \Delta V_{th}^{\ 2} + b \times \Delta V_{th} \qquad (1)$$

a, and *b* are the coefficient of a polynomial fit whose units are Gy(Si)/V^2 and Gy(Si)/V respectively. They were calculated by using the data acquired during a calibration campaigns at ESTEC [4]. The parameter *b* is related to the sensitivity of the RadFET and *a* takes into account the non-linearity response of the sensor [4]. However, it is not possible to find such parameters so that the goodness of the fit is appropriate along the full range of the TID measurement. Thus, lookup tables, based on the correspondence between the threshold voltage and the dose measured at ESTEC, are used in the final application, to convert the electrical signal of the RadFET in dose. The RadFETs were further evaluated through benchmark measurements in mixed field environments at CERN. For the latter, two irradiation areas are currently used by the Radiation to Electronics (R2E) community [5]: CNRAD [6] and H4IRRAD [7]. The usage of different RadFET types (100nm, 400nm and 1000nm) still requires further investigation in order to fully determine the respective uncertainty levels. An overall uncertainty of 50% is applied to all LHC measurement locations. This value has been evaluated on the basis of the calibration and experimental results.

2.2 Displacement Damage – p-i-n diode

Silicon p-i-n diodes are used in forward bias for monitoring 1-MeV equivalent neutron fluence (Φ_{eq}) in the LHC accelerator. Particles interacting with the silicon p-i-n diode generate stable and non-stable defects in the silicon lattice which then act as recombination centres. This effect, leading to the reduction of both the minority carrier lifetime and the silicon conductivity [8], implies an increase of the forward threshold voltage, hereafter V_f. The monitoring of the Φ_{eq} is performed by measuring the variation of the V_f during the injection in the silicon p-i-n of a short pulse current. The non-stable defects anneal versus time. From a macroscopic point of view, it has been already shown in [3] that for forward bias p-i-n diodes the voltage (V_f) measured at constant current decreases versus time after the irradiation, indicating an annealing effect. The self-heating of the injected current is to reduce, since it can further increase the annealing effect. The p-i-n diodes are not thermalized. On the RadMon, the forward current is injected through the diode during 30 ms, each 1 second with a duty cycle of 3%. Moreover, the higher the fluence is, the more significant the self-heating effect is [9]. Since the current duty cycle is low and the total 1 MeV equivalent neutron fluence in LHC is rather low (few 10^{12} n_{eq}/cm^2), the self-heating effect does not play a significant role for radiation damage annealing

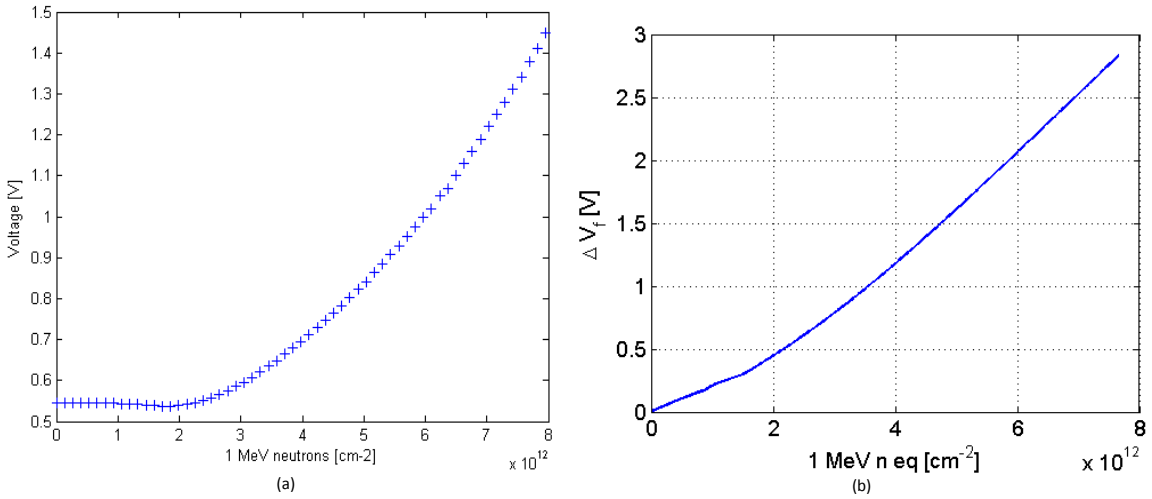

Fig. 3: Radiation responses of the silicon p-i-n diode. (a) The diode's forward voltage V_f of one p-i-n diode measured at a constant current pulse is plotted versus 1-MeV neutron equivalent fluence (Φ_{eq}) to show the measurement principle. (b) Radiation response of 3 p-i-n diodes in series after pre-irradiation of about 4×10^{12} n_{eq}/cm^2. This shows the use of the diodes as it is on the RadMon system. The parameter ΔV_f, variation of the forward voltage with respect to its initial value, is plotted versus 1-MeV equivalent fluence.

during measurement and can be neglected for the use of those p-i-n diodes in our application. This reading method has been also used for monitoring high fluences in LHC experiments as it is detailed in [9]-[11] and as it is shown in [12] for the first results at the TOTEM experiment. In Fig. 3(a), the forward voltage V_f of one diode is plotted as a function of 1 MeV equivalent neutron fluence Φ_{eq} to show the working principle. As it can be observed, this type of silicon p-i-n diode is not sensitive to radiation damage for fluences lower than few 10^{12} n_{eq}/cm^2. Therefore, the diodes used on the RadMon, were pre-irradiated up to $4x10^{12}$ cm^{-2} for monitoring lower fluence. This method allows bringing them to the working point, where the device starts to be sensitive. The variation ΔV_f, of the V_f with respect to its initial value, $V_{f\text{-}pre\text{-}irr}$, registered at the pre-irradiation stage of $4x10^{12}$ $n_{eq}cm^{-2}$, is used as monitoring parameter (2).

$$\Delta V_f = V_f - V_{f-pre-irr}(n_{eq} = 4x10^{12} cm^{-2}) \qquad (2)$$

In the RadMon system, the forward voltage of 3 silicon p-i-n diodes in series is measured to further increase the total sensitivity. As a matter of fact, the series of three p-i-n diodes will imply a higher variation of V_f for a given increase of Φ_{eq}. Fig. 3(b) depicts ΔV_f as a function of Φ_{eq} for a series of 3 pre-irradiated p-i-n diodes. The x axis starts from 0 cm^{-2} since the pre-irradiation fluence is not considered. The use of 3 p-i-n diodes in series does not deeply affect the systematic errors. As far as the bias voltage is concerned, it has been reported in [11] that the sample-to-sample accuracy of V_f after the pre-irradiation is in the order of few % (statistics made over 100 devices) thus showing a negligible effect on the error introduced. Moreover, the response curve has been evaluated by irradiating a series of three p-i-n diodes. The variation between the responses of the single p-i-n diodes could affect the response curve, indeed. Nonetheless, the results of the calibration campaign show that the spread among samples is not significant [13]. On this basis, offset and gain errors are not predominant. For monitoring the equivalent fluence, a calibration factor k (cm^{-2}/mV) from a linear fit can be applied to relate the

parameter ΔV_f (2) to Φ_{eq}, the 1-MeV neutron equivalent fluence in n_{eq}/cm^2, as it is shown in Eq. 3:

$$\phi_{eq} = k \times \Delta V_f \qquad (3)$$

The k-factor, based on a linear fit, turns out to be about 2.6×10^9 cm^{-2}/mV. However, the use of a linear curve to represent the voltage shift with respect to the 1MeV-neutron fluence (3), recently investigated for a number of pre-irradiated p-i-n diodes in [13], can be source of significant errors due to the fit function at low fluence. A look-up table, based on the correspondence between ΔV_f and Φ_{eq}, measured in [13], will be used in the final application to convert the electrical parameter of the p-i-n diodes in 1 MeV equivalent neutron fluence. The observed remaining non-linearity suggests that future pre-irradiations have to be carried out at higher levels (>4×10^{12} n_{eq}/cm^2). An overall uncertainty of 50% is applied to all LHC measurement locations. This value has been evaluated on the basis of the calibration and experimental results.

2.3 Single Event Upsets – SRAM memory

When an SRAM memory cell is exposed to ionizing radiation, the energy deposited by a single ionizing particle may be sufficient to change the state of the memory cell. This effect is commonly referred to as a Single Event Upset (SEU). The number of SEUs induced in the SRAM memory is proportional to the incoming particle fluence. The ratio of number of induced SEU over the particle fluence defines the sensitivity of the memory. Thus, a SRAM memory can be utilized as radiation monitor if its sensitivity is constant and large enough for appreciating the variation of incoming particles fluence to satisfy the requirements of a given application. The sensitivity of the SRAM memory depends on the bias voltage. Reducing the bias voltage of an SRAM memory cell will lead to a proportional decrease in the charge stored at its sensitive node, and consequently also the critical charge that must be overcome to induce a SEU. This will increase the sensitivity of the SRAM memory when operated at a reduced bias voltage. Furthermore, the sensitivity of a SRAM memory varies according to the energy of the incoming hadron particles. In addition, due to the presence of ^{10}B from the formation of boron-doped phosphosilicate glass (BPSG) dielectric, some SRAM devices can also be sensitive to thermal neutrons [14]-[15]. All those aspects are to consider for the LHC radiation environment where SEUs are induced through nuclear interactions in the device material from incoming High Energy Hadrons (HEH) or thermal neutrons (Th). To measure those fluences the RadMon is equipped with four 4 Mbit SRAM devices from Toshiba (0.4 μm,TC554001AF-70L) [16], a commercial device which does not present a SEU hardened design. That SRAM memory becomes significantly more sensitive to thermal neutrons when operated at 3V compared to 5V. The SEU cross section of the memories, for the thermal neutrons and the high energy hadrons, at the two different voltages, have been evaluated by means of radiation test in external radiation facilities [14]-[15] (Table I). The RadMon has an SEU cross section for high energy hadrons in the order of 10^{-14} cm^2/bit. With a total memory size of 16 MBits the sensitivity results to be about 10^6 n/cm^2. That sensitivity is large enough to use the TOSHIBA memory as radiation monitor in the LHC environment. The sensitivity to thermal neutrons is higher when the memory is operated at 3 V (10^{-13} cm^2). The uncertainty, indicated in brackets for each case

TABLE I
MEASURED SEU CROSS SECTIONS FOR THERMAL NEUTRONS AND HIGH ENERGY HADRONS. ERRORS INCLUDE COUNTING STATISTICS AND UNCERTAINTIES RELATED TO THE BEAM CALIBRATION

Bias	SEU cross section, σ_{SEU} (±Err) [cm^2/bit]	
	Thermals Neutrons	High energy hadrons
3 V	1.7×10^{-13} (0.4)	6.6×10^{-14} (1.7)
5 V	3.1×10^{-15} (0.8)	2.9×10^{-14} (0.7)

of Table I, is mainly due to a spread in the SEU cross section between individual Toshiba SRAM devices and it turns out to be about 25%. This is considered acceptable for the LHC monitoring purpose. Since the LHC environment is characterized by a mixed radiation field, it is important to distinguish between the contribution of high energy hadrons and thermal neutrons. It is possible to approximate the relation between number of SEUs in the chip and the respective fluence as explained in [14]. The uncertainty of the method, evaluated by using the uncertainty propagation law, depends on the relative difference between the SEU counts measured at 3V and 5V and it has been discussed in [14]-[15]. An overall uncertainty of 50% is applied to all LHC measurement locations. This value has been evaluated on the basis of the calibration and experimental results [14]-[15].

3. Software architecture

The RadMon controls software communicates with the monitoring devices located in the underground tunnel over a WorldFIP fieldbus [17]. A total of 24 fieldbus segments, with a maximum of 32 monitors, constitute the basis of the system architecture (Fig. 4). Each WorldFIP segment is connected to Front End Computer (FEC) that acts as the bus arbitrator for the segment. The Radiation Monitoring C/C++ application (RadMon) has been developed in the FESA [18] framework (Front End Software Architecture). The FESA class carries out the

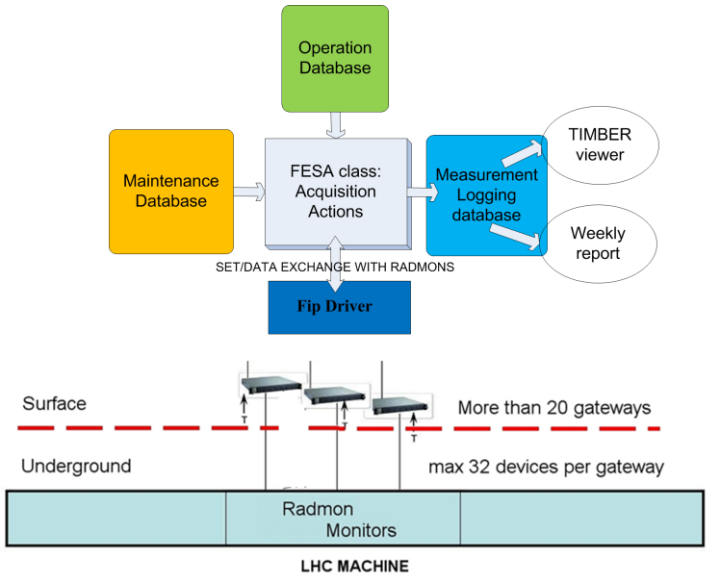

Fig. 4: Architecture of the Control and reading software.

acquisition actions of an entire segment by means of the FIP driver which provides the low level communication with the single radiation monitoring devices. The main settings of the radiation monitoring system are kept in the *Operation Database* (Fig. 4). Each radiation monitor has a unique hardware address which is used as a key field in the database acting as a link to the monitor settings (e.g. memory voltage) and to the associated types of sensors (e.g. RadFET thickness and batch) with their calibration factors and initial voltage threshold. Upon boot time, the FECs upload all the information the FESA class performs the association between hardware address and calibration data to interpret the raw data correctly. The maintenance database keeps trace of the TID received by the monitors in order to foresee the technical interventions before reaching the hardware life time. During operation, data from the monitors are stored on line in a database, named the "Measurements database". The data in the measurement database is stored for a period of one week with a time resolution of 1 second. A subset of the data from the measurement database is stored on a long term basis in the so-called "Logging database".

4.Experimental results

As discussed in the Section 2, the results of each measurement method are characterized by an uncertainty that has been quantified to be within a factor 2. This factor comes out by the calibration campaigns on the single sensors and by the usage of the RadMon in the CERN mixed radiation facilities CNRAD and H4IRRAD, and in the LHC itself, where our terms of comparison are the FLUKA calculations and other sensors which are also affected by uncertainty [14]. In fact, it is not an easy task to have accurate FLUKA calculation in very large volumes. Such comparisons suggest that the uncertainty factor 2 is enough conservative, and satisfying for the LHC measurement purposes [15]. In this Section, the use of the RadMons in CNRAD, H4IRRAD, as well as in the LHC tunnel is presented by high lightening the main results.

4.1CNRAD

The parasitic radiation test area "CNRAD" is located in a technical gallery located parallel to the main CNGS target area. At CNGS, two 400 GeV/c SPS primary beam extractions separated by 50 ms, each of them with 10,5 μs length and 2.4×10^{13} protons, impinge on a long graphite target with a cycle of 6 seconds. Parasitically located with respect to the neutrino production, the facility aims at obtaining a mixed radiation field produced by the interaction between the SPS primary beam and the target. This field will be referred as secondary beam in the following. In particular, the interaction between the secondary beam and the reflector will induce a mixed particle field in the two tunnel side galleries, named TSG45 and TSG46. Several positions inside the side gallery and both TSG(45-46) have been calibrated using the RadMon systems. TID (green), 1-MeV neutron equivalent fluence (beige) and the SEU counts (red) have been evaluated for each position as it is shown in Fig. 5 for one of the monitored locations. The SEU counters are used to evaluate the HEH and thermal neutron fluence as described in [15]. The performance of the RadMon used in CNRAD and other locations allows measuring the radiation levels within a factor of about 2.

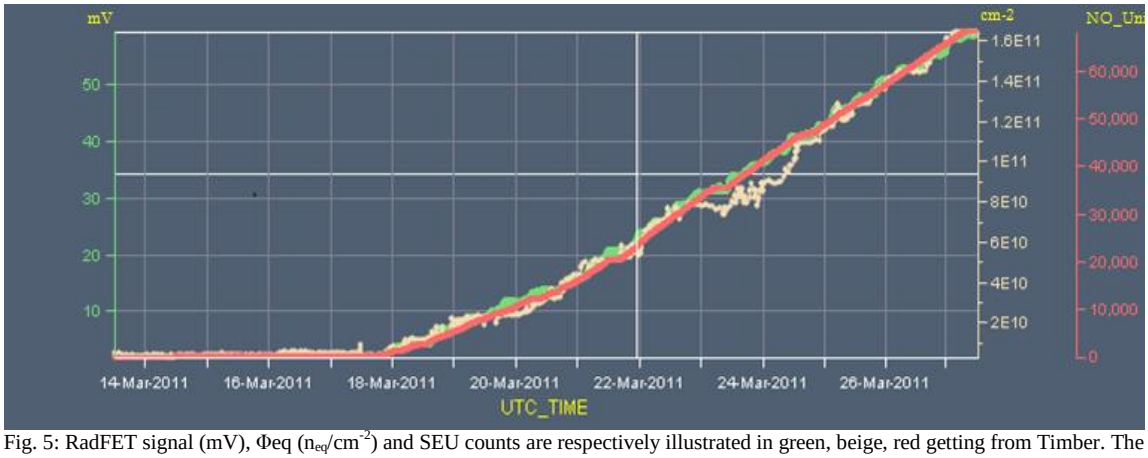

Fig. 5: RadFET signal (mV), Φeq (n_{eq}/cm^{-2}) and SEU counts are respectively illustrated in green, beige, red getting from Timber. The SEU counters are used to evaluate the HEH and thermal neutron fluence as described in [15].

4.2 H4IRRAD

Due to the difficulties related to the operation of the CNRAD test area (access possible only during technical stops, no control of the beam), within the Radiation to Electronics (R2E) Mitigation Project [5], the creation of a novel test area has been proposed, where these impediments could be partially lifted. The H4IRRAD test area setup in June 2011 in the CERN's North Area, uses a 280 GeV/c secondary proton beam from the SPS, impinging on a copper target, producing a secondary radiation field for equipment testing [7]. The most resistant commercial off the shelf (COTS) system used in the LHC tunnel and shielded areas have a failure cross section of around 10^{-9} cm^2. By assuming that an equipment is tested with a cumulated fluence of few 10^{10} cm^2/week – which corresponds to the maximum annual high energy hadrons for a nominal LHC operation in shielding areas, where COTS electronics is located – after 1-2 weeks of testing, the probability of failure is representative of a realistic scenario. The RadMon system has been used to monitor the radiation field in two locations, named internal and external irradiation zones. Table II(A) summarizes the radiation levels at different locations obtained from FLUKA simulations in terms of HEH fluence, dose in Silicon, and 1 MeV equivalent fluence (Φ_{eq}). Those radiation levels can be accumulated during 1 week of continuous operation, assuming 1 pulse of 10^9 protons every 44s SPS cycle time. A comparison between FLUKA simulations and RadFET measurements for the two slots of H4IRRAD is shown in Table II(B). An agreement in the order of ~20-30% (depending on the

TABLE II
(A) RADIATION LEVELS/WEEK AT H4IRRAD FOR TID, DD AND HEH FLUENCE AT THE DIFFERENT TEST LOCATIONS
(B) COMPARISONS OF THE RADFET MEASUREMENTS AND THE FLUKA SIMULATIONS

Testing Position	HEH ($week^{-1}.cm^{-2}$)	Dose ($Gy.week^{-1}$)	Φ_{eq} ($week^{-1}.cm^{-2}$)
Internal (ide)	5.9×10^{10}	4.8×10^{1}	3.9×10^{11}
External (side)	7.8×10^{9}	3.0×10^{0}	3.7×10^{10}
External (downstream)	5.1×10^{9}	2.3×10^{0}	1.8×10^{10}

(A)

H4IRRAD Slot	Fluka (Gy(Si))	Measurement (Gy(si)
1st Slot	5.6×10^{1}	4.6×10^{1}
2nd Slot	1.28×10^{2}	1.0×10^{2}

(B)

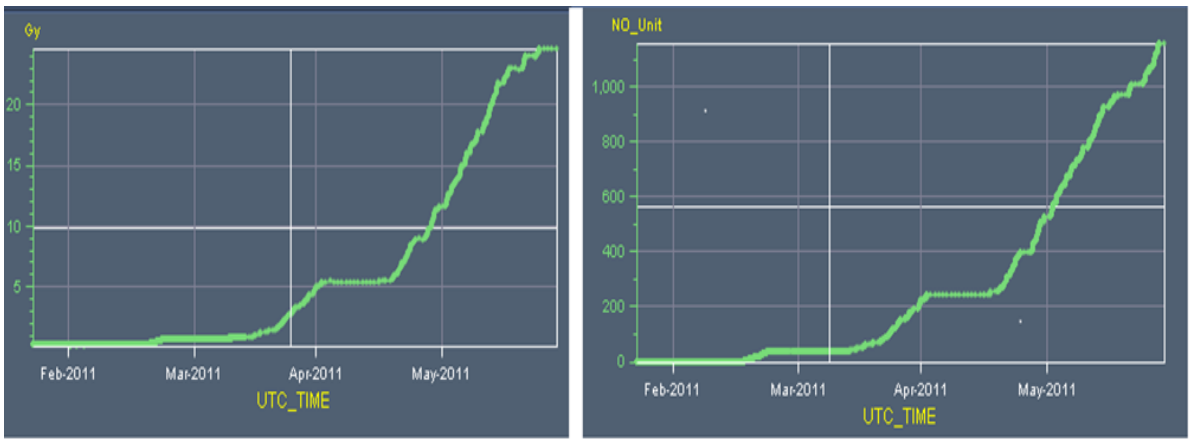

(a) (b)

Fig. 6: Measurement of the TID in a tunnel location (A) and of the SEU counts in a shielded area (B) for the first 5 months of the 2011.

location) between FLUKA simulations and measurements by RadMon was obtained for both the 1st and the 2nd measurement slot (June 2011 and July 2011). Results are very satisfying since the experience confirmed that the RadMon system can be used in the test areas by assuming a factor 2 of uncertainty. Moreover, those tests allow understanding deeply the calibration of the sensors in high energy mixed particle field, which is useful for the LHC monitoring, since the radiation field is similar.

4.3 LHC monitoring

The RadMon detectors are used all around the LHC ring, in both tunnel areas as well as in adjacent shielded areas, to monitor the radiation levels during LHC operation. Currently in the LHC, about 400 RadMons, are continuously read out at a rate of one Hertz. SRAM memories on the RadMon system are operated at 5V (lower sensitivity) in tunnel locations, as elevated radiation levels are expected. On the contrary memories are operated at 3V (higher sensitivity) when RadMons are employed in shielded areas, where during early LHC operation the cumulative yearly fluence hardly overcome 10^7 HEH/cm^2/year. Thus, the sensitivity needs to be higher than the one in tunnel locations. However, due to the high sensitivity of the memory to the thermal neutrons when operating at 3 V, two measurements are needed to evaluate the HEH and thermal neutrons fluence, as explained in section 2.3 and [15]. Fig. 6(a) reports an example of the measurement of the TID in a tunnel location. Fig. 6(b) reports the cumulated SEU count of the SRAM memories of a RadMon located in a shielded area. The monitoring of the SEUs allowed correlating sudden failures of commercial electronics to the radiations. In particular, the increase of the TID allows understanding the drift of analog parameters of the electronic boards installed in the tunnel. Within the framework of the R2E Mitigation Project [5], the RadMons are used – together with the beam loss monitors (BLM) – to produce a weekly report [19], in which the cumulated high energy hadron fluence is evaluated for critical locations where sensitive electronic equipments are used. The most meaningful data were obtained in 2011; thus, they are not yet published. Those reports allow correlating observed radiation induced equipment failures with the respective accumulated radiation levels, to plan the required mitigation strategies.

5.Conclusion

The RadMon detector, conceived to measure the radiation levels leading to possible damage of electronics installed in the LHC tunnel and its adjacent shielded areas, anticipate possible device degradation and identify instantaneous failures of the electronic equipments, has been presented. The working principle and the rationale of the used sensors for monitoring the TID, 1-MeV equivalent fluence and HEH fluence in the experimental test areas, LHC tunnel and shielded locations have been described. The sensors have been characterized in referenced calibration facility such as ESA/ESTEC (Co60 source) [4], CEA-PROSPERO (1 MeV neutron equivalent fluence) [13], and PSI (proton beam) [14] in order to determine their response curves, sensitivities, measurement ranges, and uncertainties. During all sensor calibration campaigns (RadFET, p-i-n diodes and memories), the full RadMon device and readout system has been used to allow for fast and reliable measurements, providing in parallel the three radiation parameters. Additional cross calibration measurements have been performed with the ESA SEU counter [20]. Finally, the RadMon device has been appreciated by those facilities, and, in particular, it was used during PSI radiation test campaigns as a fast cross-check of the given radiation, at CEA for online calibration of the radiation field, and similar activities are planned for the Jefferson LAB in Virginia. Those calibrations have been also applied to a mixed radiation field in CERN experimental areas, such as CNRAD and H4IRRAD. The important calibration efforts, together with the good coverage of monitors in the LHC accelerator, successfully allowed for a detailed monitoring of the LHC underground areas during the first two years of operation. It allowed confirming electronics failures due to radiations, relating them to the observed radiation levels, and providing detailed bench-marks for the FLUKA calculations. An overall uncertainty of a factor 2 has been reached which is remarkable in such complex environment. Further investigations are under study to try an improvement of that performance. New sensors will be analysed, calibrated, and then tested in the LHC environment.

References

[1] T. Wijnands, C. Pignard, R. Tesarek, *An on line radiation monitoring system for the LHC machine and experimental caverns,* 12th Workshop on Electronics for LHC and Future Experiments, Valencia, Spain (2006) pp. 113-118. Available also on http://cdsweb.cern.ch/record/1027423.

[2] A. G. Holmes-Siedle and L. Adams, *Handbook of radiation effects*, 2nd ed., Oxford University Press, New York 2002.

[3] F. Ravotti, *Development and Characterization of radiation monitoring sensors for the high energy physics experiments of the CERN LHC accelerator*, *CERN thesis collection*, PhD thesis, Dept. Electronics, Univ. Montpellier II, CERN-THESIS-2007-013, Montpellier, France, (2006). cdsweb.cern.ch/record/1014776/files/thesis-2007-013.pdf.

[4] G. Spiezia, C. Pignard, S. Batuca, D. Kramer, *ESTEC test 21.06.2010 – RadFET Calibration*, CERN report, (2010). Documentation available at: https://edms.cern.ch/nav/CERN-0000083951%26expand_open=Y in the tag *Radiation Test Report/ESTEC.*

[5] CERN Radiation to Electronics mitigation project (R2E). https://r2e.web.cern.ch/R2E/

[6] CNRAD. *CERN experimental test area for Radiation to Electronics Project.* All documentation available at: http://radwg.web.cern.ch/RadWG/Pages/CNRAD/cnrad_frame.htm

[7] B. Biskup et al., *Commissioning and Operation of the H4IRRAD Mixed-Field Test Area*, CERN-ATS-Note-2011-121 PERF, (2011). Note available on: http://cdsweb.cern.ch/record/1403188

[8] A. B. Rosenfeld et al., *P-I-N diodes with a wide measurement range of fast neutrons doses, Radiat. Prot. Dos.*, **101.1/4** (1990), 175-178.

[9] J. Mekki, *Characterization and performance optimization of radiation monitoring sensors for high energy physics experiments at CERN LHC and Super-LHC*, PhD thesis, Dept. Electronics, Univ. Montpellier II, CERN-THESIS-2009-180, Montpellier, France, 2009. *cdsweb.cern.ch/.../CERN-THESIS-2009-180.pdf.*

[10] J. Mekki, M. Moll, M. Fahrer, M. Glaser and L. Dusseau, *Prediction of the response of the commercial BPW34FS silicon p-i-n diode used as radiation monitoring sensors up to very high fluences*, IEEE Trans. Nucl. Sci., **57** (2010) 2066-2073.

[11] F. Ravotti, M. Glaser, M. Moll, Sensor Catalogue – *Data compilation of solid-state sensors for radiation monitoring*, CERN TS-Note 2005-002 (2005).

[12] F. Ravotti on behalf of the TOTEM collaboration, *First Radiation Background Studies for the TOTEM Roman Pot and T2 Detectors*, Paper NP3.M-50 in Proc. IEEE Nuclear Science Symposium (NSS/MIC 2011), Valencia, Spain, October 23-29, 2011, to be published, (2012).

[13] G. Spiezia, X. Jacquet, *RADMON test – CEA*, CERN report, (2011), Documentation available at: https://edms.cern.ch/nav/CERN-0000083951%26expand_open=Y in the tag *Radiation Test Report/CEA.*

[14] K. Røed, M. Brugger, D. Kramer, A. Masi, P. Peronnard, C. Pignard, and G. Spiezia, *Method for measuring mixed field radiation levels relevant for SEEs in the LHC.* To be published in the proc. on the RADECS conference, Sevilla, Spain, (2011).

[15] D. Kramer *et al.*, *LHC RadMon SRAM detectors used at different voltages to determine the thermal neutron to high energy hadron fluence ratio*, IEEE Trans. Nucl. Sci., **58** (2011) 1117-1122.

[16] Toshiba – *Toshiba MOS Digital Integrated Circuit Silicon Gate CMOS* – Datasheet available on : http://www.datasheetcatalog.org/datasheet/toshiba/1814.pdf

[17] WorldFIP. All documentation available on : http://www.worldfip.org

[18] M. Arruat et al., *Front-End Software Architecture*, ICALEPCS 2007.

[19] Radiation levels in the LHC related to the R2E mitigation project: All documentation available on: http://radwg.web.cern.ch/RadWG/

[20] R. Harboe-Sorensen et al., *The Technology Demonstration Module On-Board PROBA-II, IEEE Trans. Nucl. Sci.*, **58** (2011) 1001-1007.